Hydrodynamic Evidence in Support of Spacer Regions in Chromatin

Abstract. *Quasi-elastic light scattering and sedimentation velocity methods were used to study the hydrodynamic properties of purified dimer subunits obtained from partial digestion of chicken erythrocyte chromatin with staphylococcal nuclease. The experimental value of 1.87 ± 0.08 × 10^{-7} gram per second for the friction factor of these dimer subunits in low ionic strength buffer cannot be reasonably interpreted in terms of a contiguous sphere model. Analysis by means of an equivalent dimer method suggests that the spacer region accounts for a maximum of 19 percent of the friction properties of the dimer.*

Partial nuclease digestion of chromatin from mammals (*1*, *2*), yeast (*3*), plants (*4*), and other eukaryotes (*5*) has shown that nuclease-resistant regions are periodically organized along the chromatin strand into subunits that have been called ν bodies (*6*), nucleosomes (*7*), and PS particles (*1*). Kornberg (*8*) and Van Holde *et al.* (*9*, *10*) proposed two models in which the repeat unit consists of a short DNA segment and a core of two each of the histone proteins H2A, H2B, H3, and H4. In the Van Holde model only part (~ 140 base pairs) of the DNA repeat unit is wrapped around the eight-histone core nucleus (*9*, *11*). This tightly associated octameric histone-DNA complex has been called a core-particle (*10*, *12*). The remaining 20 to 60 base pairs of nuclease accessible DNA (*10*, *11*, *13*) in the subunit serves as a bridge (*9–11*) to link core particles into a "bead and bridge" pattern (or structure), as observed by electron microscopy (*6*, *11*). Within this framework of the beads and bridge model (*6*, *9*, *11*), one may view the structure of chromatin fibers either as a set of contiguous subunits having collapsed bridge regions of DNA [where the diameter of the beads is comparable to that of the isolated core particle, that is, 100 Å (*9*, *10*, *14*)] or as a series of core particles linked by extended bridge or spacer regions of DNA (*15*). Indeed, it is likely that chromatin could exist as both contiguous and noncontiguous regions, depending on the nature of the nonhistone proteins, lysine-rich histone proteins, and polycationic species that are associated with the bridge region on a local level (*15*). Small changes in the proteins present or in the ionic strength could influence the rigidity and extensibility of the bridge regions, and consequently that of the chromatin fiber.

Our studies have been directed toward using hydrodynamic and light-scattering techniques to determine whether chromatin subunits in solution exist as either contiguous beads or as beads having extended bridge conformation. Whereas electron micrograph (*6*, *11*, *16*) and chemical (*10*, *13*) evidence for the existence of bridge regions has been reported, few physical measurements on multimers of chromatin subunits have been carried out. Quasi-elastic light-scattering measurements coupled with hydrodynamic techniques should provide detailed information regarding the conformation of multimers of chromatin subunits. The superstructure of nucleosomes is still a matter of speculation. The general consensus, however, is that polymeric nucleosomes form a helical structure (*17–19*), although alternative conformations, that is, random coils or rods, may be equally feasible for data interpretation (*17*, *19*). The inability to distinguish between the various structures for the multimeric units is due, in part, to the number of parameters (*20*). The additional parameter representing a spacer region would further complicate the interpretation. Structural studies of dimers, a unit common to all super-

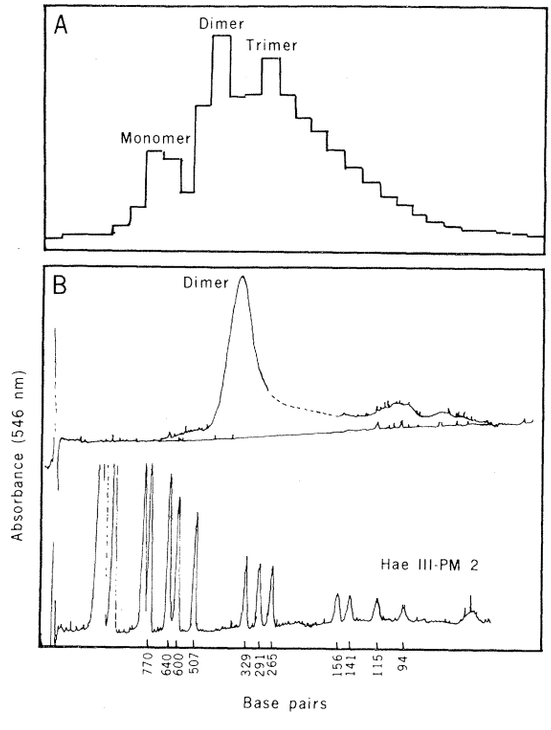

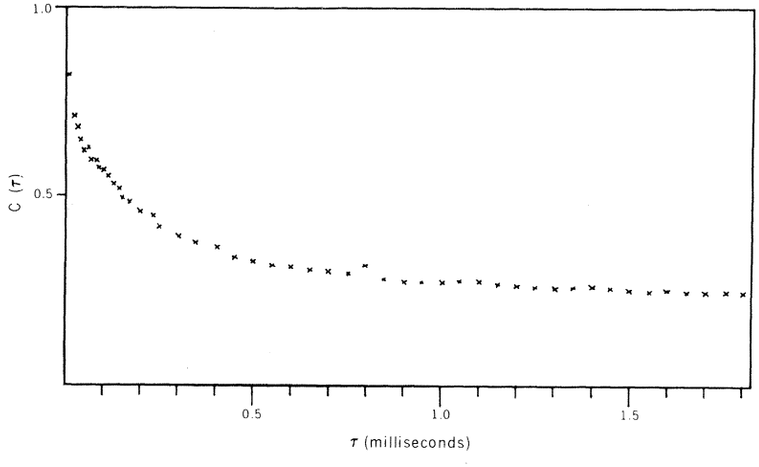

Fig. 1 (left). (A) Isopycnic sucrose gradient separation of chicken erythrocyte chromatin multimers. Multimeric chromatin subunits (two fractions totaling 5.7 ml and comprised of monomer, dimer, and trimer subunits) that were obtained from a Bio-Rad A-5m column 80 cm long and 2.5 cm in diameter (*21*) were combined, concentrated, and further separated on an isopycnic sucrose gradient (ρ = 1.51 (*29*). The optical density profile shown consists of monomer, dimer, and trimer components. The dimer fraction used is indicated by the arrow. (B) Electrophoretic pattern of DNA obtained from the dimer. The DNA obtained after incubation of the dimer fraction with pronase and sodium dodecyl sulfate was subjected to electrophoresis on a 3½ percent polyacrylamide gel (27 cm long) according to Loening (*30*). A Hae III digest of PM2 DNA was run simultaneously, and both gels were stained with toluidine blue and scanned at 546 nm in a Gilford Model 2400 gel scanner. The latest size calibration of the PM2 Hae III fragments as determined by Kovacic and Van Holde (*31*) are indicated on the abscissa. Fig. 2 (above). Representative autocorrelation function for chromatin dimer. The autocorrelation function for dimer particles of chromatin was analyzed as a single exponential decay function of the form $C(\tau) = A \exp(-2DK^2\tau) + B$ where $K = (4\pi n/\lambda_0) \sin(\theta/2$; B is the baseline, and $A + B = 1$. The data were collected at 0.5°C in the range $40° \leq \theta \leq 70°$.

structure conformations, should provide more precise information regarding the bead separation.

Using quasi-elastic light-scattering techniques, we have determined the friction factor f for dimers of chicken erythrocyte chromatin. The preparation and isolation of chicken erythrocytes has been described (*10, 21*). Nuclei were digested by micrococcal nuclease at 37°C, and the digestion was terminated by making the solution 10 m*M* in EDTA and cooling on ice. The nuclei were centrifuged at 12,000*g* for 15 minutes, resuspended in 10 ml of a solution of 10 m*M* tris-HCl, *p*H 7.5, and 0.7 m*M* EDTA, and disrupted briefly on a Virtis homogenizer at medium setting (*22*). After centrifugation of the nuclear debris, the supernatant was made 7 percent in sucrose and applied to a Bio-Rad A-5m column (90 by 2.5 cm) equilibrated with 10 m*M* tris-HCl and 0.7 m*M* EDTA, *p*H 7.5, at 5°C. The dimer particles were purified on isopycnic sucrose gradients (Fig. 1A) and, after dialysis in 10 m*M* tris-HCl, 0.7 m*M* EDTA, *p*H 7.5 buffer, were characterized by circular dichroism (not shown), sedimentation velocity (= 16.2*S* in 10 m*M* tris-HCl, *p*H 7.5), gel electrophoresis of the extracted DNA (Fig. 1B), and quasi-elastic light-scattering experiments. The last-mentioned studies were carried out as described (*23*). The samples were filtered by gravity flow into the scattering cell in the cold room and kept cold by circulating ice water while the data were collected (*24*). The autocorrelation functions exhibited single exponential decay (Fig. 2) with the homodyne decay constant $1/\tau$ (*25*)

$$1/\tau = 2D(4\pi n/\lambda_0)^2\sin^2(\theta/2) \qquad (1)$$

where D is the translational diffusion coefficient, n is the index of refraction, λ_0 is the wavelength (488 nm) of incident light, and θ is the scattering angle. The translational diffusion coefficient for the dimer obtained by this method, corrected to 20°C, was $D = (2.16 \pm 0.10) \times 10^{-7}$ cm²/sec, or $f = kT/D = (1.87 \pm 0.08) \times 10^{-7}$ g/sec for the friction factor f at 20°C (*26*).

The effective hydrodynamic radius R for the friction beads (core particle) for contiguous spheres is computed from above to be (*27*)

$$R = f/8\pi\eta \simeq (74.4 \pm 3.2) \times 10^{-8}\,\text{cm} \qquad (2)$$

where $\eta = 0.01$ poise at 20°C. This value is considerably larger than the reported values of $R = 50$ to 55 Å for the nucleosome (*6, 7, 9–11, 14, 16*). The additional asymmetry exhibited by the dimer is presumed to be the result of a bridge region (*27, 28*). If it is assumed that the center-to-center distance B is comprised of the core particle contribution ($2R = 100$ Å) plus the minimum 40 base pairs at a separation of 3.4 Å per base pair, then the minimum separation distance is $B_m = 236$ Å, which results in an effective friction bead radius (*19*)

$$R' = f/(12\pi\eta - f/B_m) = 62.8 \times 10^{-8}\,\text{cm} \qquad (3)$$

All the frictional properties of the hypothetical hydrodynamically equivalent dimer are contained in the beads of radius R' separated by a frictionless spacer region. The upper limit to the contribution of the actual spacer region to the frictional properties of the dimer is estimated to be $(R' - R)/R \simeq 0.19$, where $R = 50$ Å (*28*). This excess contribution is reduced to ~ 5 percent if the maximum (60 base pairs) is used in the calculation. We emphasize that the dimers used in our low ionic strength studies contained lysine-rich histones, which may influence the rigidity of the spacer region. A flexible spacer at higher ionic strength may result in a collapse to the contiguous bead model.

KENNETH S. SCHMITZ
Department of Chemistry, University of Missouri, Kansas City 64110
BARBARA RAMSAY SHAW
Department of Chemistry, Duke University, Durham, North Carolina 27706

References and Notes

1. R. Rill and K. E. Van Holde, *J. Biol. Chem.* **248**, 1080 (1973); C. G. Sahasrabuddhe and K. E. Van Holde, *ibid.* **249**, 152 (1974).
2. M. Noll, *Nature (London)* **251**, 249 (19 → D. R. Hewish and L. A. Burgogne, *Biochem. Biophys. Res. Commun.* **52**, 504 (1973).
3. D. Lohr and K. E. Van Holde, *Science* **188**, 165 (1975).
4. J. D. McGhee and J. D. Engel, *Nature (London)* **254**, 449 (1975).
5. M. A. Gorovsky and J. B. Keevert, *Proc. Natl. Acad. Sci. U.S.A.* **72**, 3536 (1975); B. M. Honda, D. L. Baillie, E. P. M. Candido, *FEBS Lett.* **48**, 156 (1974).
6. A. L. Olins and D. E. Olins, *Science* **183**, 330 (1974).
7. P. Oudet, M. Gross-Bellard, P. Chambon, *Cell* **4**, 281 (1975).
8. → R. D. Kornberg, *Science* **184**, 868 (1974).
9. → K. E. Van Holde, C. G. Sahasrabuddhe, B. Ramsay Shaw, *Nucleic Acids Res.* **1**, 1579 (1974); K. E. Van Holde and I. Isenberg, *Acc. Chem. Res.* **8**, 327 (1975).
10. K. E. Van Holde, B. Ramsay Shaw, D. Lohr, T. M. Herman, R. T. Kovacic, *Proc. FEBS Meet.* **10**, 57 (1975); B. Ramsay Shaw, T. M. Herman, R. T. Kovacic, G. S. Beaudreau, K. E. Van Holde, *Proc. Natl. Acad. Sci. U.S.A.* **73**, 505 (1976).
11. K. E. Van Holde, C. G. Sahasrabuddhe, B. Ramsay Shaw, E. F. J. VanBruggen, A. C. Arnberg, *Biochem. Biophys. Res. Commun.* **60**, 1365 (1974).
12. The entire subunit of 200 base pairs DNA plus the eight-histone core has been generally referred to as a nucleosome. We use the term core or core particle to designate only that fraction of DNA in the subunit that is tightly associated with the octameric histone complex as revealed by nuclease digestion. The length of DNA in the core particle is nearly invariant (~ 140 base pairs), whereas the length of DNA in the bridge regions that connect core particles has been found to vary as much as 50 base pairs from one organism to another [→ D. Lohr, J. Corden, K. Tatchell, R. T. Kovacic, K. E. Van Holde, *Proc. Natl. Acad. Sci, U.S.A.*, **74**, 79 (1977)].
13. B. Sollner-Webb and G. Felsenfeld, *Biochemistry* **14**, 2916 (1975); R. Axel, *ibid.*, p. 2921; R. T. Simpson and J. P. Whitlock, Jr., *Nucleic Acids Res.* **3**, 117 (1976); A. J. Varshavsky, V. V. Bakayev, G. P. Georgiev, *ibid.*, p. 477.
14. J. F. Pardon, D. L. Worcester, J. C. Wooley, K. Tatchell, K. E. Van Holde, B. M. Richards, *Nucleic Acids Res.* **2**, 2163 (1975).
15. B. Ramsay Shaw, T. M. Herman, R. T. Kovacic, K. E. Van Holde, in *ICN-UCLA Symposia on Molecular and Cellular Biology*, D. P. Nierlich, W. J. Rulter, C. F. Fox, Eds. (Academic Press, New York, 1976), vol. 5, p. 13.
16. C. F. Woodcock, *J. Cell Biol.* **59**, 737a (1973); J. P. Langmore and J. C. Wooley, *Proc. Natl. Acad. Sci. U.S.A.* **72**, 2691 (1975).
17. R. D. Carlson and D. E. Olins, *Nucleic Acids Res.* **3**, 89 (1976).
18. S. Bram, G. Butler-Brown, P. Baudy, K. Ibel, *Proc. Natl. Acad. Sci. U.S.A.* **72**, 1043 (19 → J. T. Finch and A. Klug, *ibid.* **73**, 1897 (1976); R. Mandel and G. D. Fasman, *Nucl. Acids Res.* **3**, 1839 (1976).
19. B. Ramsay Shaw and K. S. Schmitz, *Biochem. Biophys. Res. Commun.* **73**, 224 (1976).
20. The helical pitch P and fiber radius F (helical center to bead center) necessarily fix the angle of inclination $\alpha = \arctan(P/2\pi F)$. If we define the center-to-center distance between adjacent beads as B, then the angle θ defined by the helical axis and adjacent bead locations on the plane perpendicular to the helical axis is given by $\theta = 2 \arcsin(B\cos\alpha/2F)$. If the bead radius is proportional to B, the entire helical structure is determined by the ratios P/F, B/F, and B/R, independent of their absolute values.
21. → B. Ramsay Shaw, J. Corden, C. G. Sahasrabuddhe, K. E. Van Holde, *Biochem. Biophys. Res. Commun.* **61**, 1193 (1974).
22. The nuclei were briefly (30 seconds to 1 minute) exposed to a minimum shearing force (medium setting, 35/110) of the Virtis 45 homogenizer in an attempt to minimize possible artifacts resulting from sample preparation. It is not possible to determine whether the state of the multimers represents the natural state of chromatin in the cell.
23. J. M. Schurr and K. S. Schmitz, *Biopolymers* **12**, 1021 (1973); K. S. Schmitz and J. M. Schurr, *ibid.*, p. 1543; W. I. Lee and J. M. Schurr, *ibid.* **13**, 903 (1974).
24. In order to determine whether the gravity flow filtration method caused substantial denaturation of the dimer, sedimentation velocity measurements were performed before and after the quasi-elastic light-scattering experiments. The values $S_{20} = 16.2$ (before) and $S_{20} = 16.7$ (after) for the dimer, as compared to $S_{20} = 6.5$ for DNA extracted from the dimer, suggest that denaturation did not occur to any significant extent (S_{20} is the sedimentation coefficient at 20°C).
25. There is an excellent series of papers reviewing the theory and applications of fluctuation spectroscopy to biological systems in D. Magde, *Q. Rev. Biophys.* **9**, 35 (1976); W. W. Webb, *ibid.*, p. 49; M. Ehrenberg and R. Rigler, *ibid.*, p. 69; L. DeMaeyer, K. G. Nadig, J. Hendrix, B. Saleh, *ibid.*, p. 83; J. M. Shurr, *ibid.*, p. 109.
26. The optical density of the samples used in the determination of D for the dimer was in the range $A_{260} = 0.28$ to 0.19 with no apparent dependence of D on concentration. For example, column fraction 12 (approximately ten core units) gave values of $D_{20} = (1.01 \pm 0.04) \times 10^{-7}$ and $(0.98 \pm 0.12) \times 10^{-7}$ at optical densities of $A_{260} = 0.275$ and 0.015, respectively (largest concentration range in our studies).
27. The Kirkwood theory [J. G. Kirkwood, *J. Poly. Sci.* **12**, 1 (1954)] for a linear string of n frictional beads of radius R results in an expression for the friction factor f,

$$f = 6\pi\eta nR/\left(1 + \frac{R}{n}\sum_{i\neq j} < 1/R_{ij} >\right)$$

where η is the solvent viscosity and $< 1/R_{ij} >$ is the average reciprocal distance between the centers of beads i and j. The friction factor for the dimer then becomes

$$f_{\text{dimer}} = 12\pi\eta R/\left(1 + \frac{R}{B}\right)$$

If the friction beads of the dimer are contiguous ($B = 2R$), then rearrangement of this expression

gives R as defined in Eq. 2. If the quantity B differs from R and can be estimated by independent means, then

$$R = f/[12\pi\eta - (f/B)]$$

The latter equation clearly indicates the effective radius R for a friction bead is reduced for increased values of B.

28. Recent data suggest that the core particle is "disklike" with a radius of 50 Å and a height of 50 Å (J. C. Wooley and J. Pardon, personal communication). The radius of the equivalent spherical volume, that is, $\pi r^2 L = (4\pi/3)R^3$, is estimated to be 45.4 Å for the dehydrated nucleosome. It is unlikely that the 74-Å radius computed from the contiguous sphere model is due to hydration alone. The value of R (50 Å) used in the calculation of B (236 Å) is representative of the hydrated nucleosome (lower limit) since this value was estimated from hydrodynamic properties of the monomer (*1*). It could be argued that the asymmetric shape of the "disklike" structure of the core particle contributes significantly to the frictional properties of the dimer. This seems unlikely, however, since f/f_0 is about 1.1 for the monomer, suggesting almost spherical symmetry (*1*). In addition, Perrin's equations require an axial ratio a/b be greater than 5 to account for a 20 percent increase in the frictional properties of either prolate or oblate spheroids. The disklike model suggests $a/b \cong 2$, in which there is only a 4 percent increase in the friction factor compared to that of an equivalent sphere ($f/f_0 = 1.04$) [K. E. Van Holde, *Physical Biochemistry* (Prentice-Hall, Englewood Cliffs, N.J., 1971), p. 81]. The equivalent sphere model can, therefore, adequately represent the hydrodynamic properties of the nucleosome.
29. M. Noll, *Nature (London)* **215**, 360 (1967); K. S. McCarty, Jr., R. T. Vollmer, K. S. McCarty, *Anal. Biochem.* **61**, 165 (1974).
30. U. E. Loening, *Biochem. J.* **102**, 251 (1967).
31. T. K. Kovacic, thesis, Oregon State University (1976); _____ and K. E. Van Holde, in preparation.
32. We thank L. Lewis and G. Riedel for technical assistance. Supported in part by grants from NSF (GP-25551 and BMS 73-06819 AO2). NIH (GM23681-01), and Research Corporation.

26 July 1976; revised 4 February 1977

1,25-Dihydroxycholecalciferol and Parathormone: Effects on Isolated Osteoclast-Like and Osteoblast-Like Cells

Abstract. *The actions of 1,25-dihydroxycholecalciferol [1,25-$(OH)_2D_3$] and parathormone, both effective bone-resorptive agents in vivo and in vitro, were tested on CT (osteoclast-like) and PT (osteoblast-like) bone cells maintained in culture. Both agents stimulated acid phosphatase activity and hyaluronate synthesis in the CT cells and decreased alkaline phosphatase, citrate decarboxylation, and collagen synthesis in the PT cells. Calcitonin inhibited the changes induced in the CT but not in the PT cells. The activity of 1,25-$(OH)_2D_3$ differed from that of parathormone in one key respect: it did not increase cellular cyclic adenosine monophosphate, whereas parathormone did. Prior incubation of the bone cells with 1,25-$(OH)_2D_3$ for 6 to 24 hours made the cells refractory to the effect of parathormone on cyclic adenosine monophosphate formation. These data suggest that 1,25-$(OH)_2D_3$ and parathormone induce bone resorption by affecting the same cell types (osteoblasts and osteoclasts) although at different cellular sites.*

Vitamin D is involved in at least two major aspects of bone metabolism—mineralization and resorption (*1–3*). Its physiologically active polar metabolite, 1,25-dihydroxycholecaliciferol [1,25-$(OH)_2D_3$] indirectly promotes mineralization of bone organic matrix by stimulating calcium and phosphate transport across the intestine to increase the concentrations of these ions at calcification sites (*3, 4*). In addition, this metabolite directly affects bone resorption in vivo (*5*) and in vitro (*6, 7*) leading to mineral release (*8*), degradation of organic matrix, and unique metabolic changes correlated with bone resorption, including decreased citrate decarboxylation (*9*) and increased lactate production (*6*).

The cellular basis for the direct effect of vitamin D_3 metabolites on bone is not known. Bone contains several different cell types. These vary from relatively undifferentiated osteoprogenitor cells to highly differentiated osteoblasts, osteocytes, and osteoclasts. Net gain or loss of bone is a result of the relative actions of these cells (*10*). Conceivably, 1,25-$(OH)_2D_3$ could affect one or all of these cells to exert its biochemical effect on bone resorption.

In order to understand the direct action of 1,25-$(OH)_2D_3$ on bone, it would seem essential to identify the cells responsive to this agent and to define the biochemical changes elicited. We have recently developed a technique that allows us to study in cell culture separate bone cell populations enriched in cells which express biochemical markers generally associated with either osteoblasts (parathormone-sensitive, or PT cells) or osteoclasts (calcitonin- and parathormone-sensitive, or CT cells) (*11–13*). We have reported (*13*) that the CT cells have high basal levels of acid phosphatase and hyaluronate-synthesizing capacity; these activities are stimulated by parathormone, and calcitonin blocks this stimulation. In contrast, the PT cells exhibit high levels of prolyl hydroxylase (*13*), collagen synthesis (*14*), citrate decarboxylation, and alkaline phosphatase

Table 1. Responses of CT and PT cells to 1,25-$(OH)_2D_3$, parathormone, calcitonin, and 24,25-$(OH)_2D_3$. Primary cultures (6 days old) of CT cells (populations 2 and 3) and PT cells (populations 5 and 6) were subdivided into multiwell tissue culture dishes containing minimum essential medium (Gibco) supplemented with 10 percent fetal calf serum (FCS) at a density of 1×10^5 cells per well. After the cells became attached to the wells overnight, 1,25-$(OH)_2D_3$ ($10^{-9}M$), parathormone ($4 \times 10^{-9}M$), calcitonin ($2 \times 10^{-9}M$), or 24,25-$(OH)_2D_3$ ($10^{-9}M$) was added in fresh FCS-supplemented medium, except when collagen synthesis was measured, in which instance the FCS was omitted. Incubation was continued for 5 minutes only for cyclic AMP formation, 44 hours for collagen synthesis, and 48 hours for the remainder of the tests. For the analysis of hyaluronate synthesis, [^{3}H]glucosamine (20 μc/ml) was present from hours 44 to 48. [^{14}C]Citrate (0.1 μc/ml) was present from hours 46 to 48 in order to measure citrate decarboxylation ($^{14}CO_2$ evolved). For the analysis of collagen synthesis, ascorbic acid (0.1 mg/ml) and [^{14}C]proline (0.4 μc/ml) were present for the entire 44-hour period. Total collagen (cells and medium) was assayed as collagenase-digestible radioactive protein. When FCS was omitted the cells ceased to divide but retained their characteristic morphology and continued to synthesize protein. These experiments were performed on five different preparations of primary cell cultures, with similar results each time. Results are expressed as disintegrations per minute per 10^5 cells for triplicate or quadruplicate samples (± standard deviation).

Cells	Control	1,25-$(OH)_2D_3$	Parathormone	Calcitonin	24,25-$(OH)_2D_3$
			Hyaluronate synthesis		
CT	13,000 ± 500	18,000 ± 1,400*	22,000 ± 2,200*	12,000 ± 570	14,000 ± 1,000
PT	15,000 ± 1,800	14,100 ± 2,000	13,000 ± 2,300	12,000 ± 1,800	(Not done)
			^{14}C-labeled collagen synthesized		
CT	54,000 ± 2,700	48,000 ± 4,600	51,700 ± 5,000	49,700 ± 6,500	51,000 ± 8,500
PT	117,000 ± 9,800	69,800 ± 800*	63,800 ± 4,900*	107,000 ± 12,000	108,700 ± 9,100
			Citrate decarboxylation		
CT	5,000 ± 500	3,500 ± 800	4,000 ± 600	5,500 ± 300	6,000 ± 1,200
PT	39,000 ± 1,400	16,000 ± 700*	18,000 ± 1,200*	33,600 ± 1,100	41,000 ± 4,800

* $P < .02$.